Algorithm document for SCIAMACHY Polar Stratospheric Cloud Detections

Date of origin: March 25, 2011

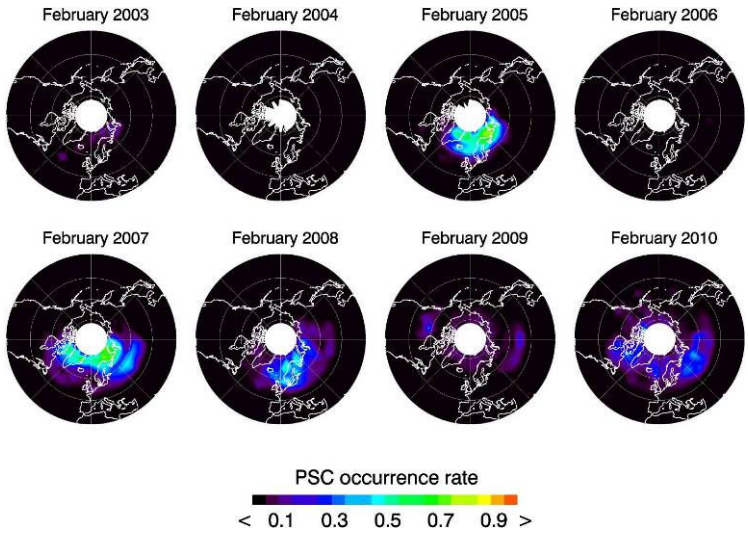

Author: Priv.-Doz. Dr. Christian von Savigny
Institute of Environmental Physics
University of Bremen
Otto-Hahn-Allee 1
28334 Bremen
e-mail: csavigny@iup.physik.uni-bremen.de

Algorithm document for SCIAMACHY Polar Stratospheric Cloud Maps

1. Polar Stratospheric Cloud detection method:

The method to detect polar stratospheric clouds (PSCs) in SCIAMACHY limb measurements is based on a colour-index approach exploiting the different relative contributions of scattering by air molecules (Rayleigh scattering) and the PSC particles at two different wavelengths. The two wavelengths are λ_1 = 1090 nm and λ_2 = 750 nm, falling in SCIAMACHY channels 6 and 4, respectively. These two wavelengths were chosen because they are not affected by molecular absorption, and because they are sufficiently large to allow sensing the lower stratosphere without the atmosphere between the tangent point and SCIAMACHY becoming optically thick. No forward radiative transfer model is required for this data product. Fig. 1 shows sample limb spectra for SCIAMACHY channels 4 and 6 with the two wavelengths used for the detection of PSCs highlighted. Rather than using limb radiance profiles for single SCIAMACHY pixels we employ limb radiance profiles (I) spectrally integrated over a wavelength range of 10 nm centred at wavelengths λ_1 and λ_2. In a first step the colour index profile $R_c(TH)$ – where TH refers to the tangent height – is determined by:

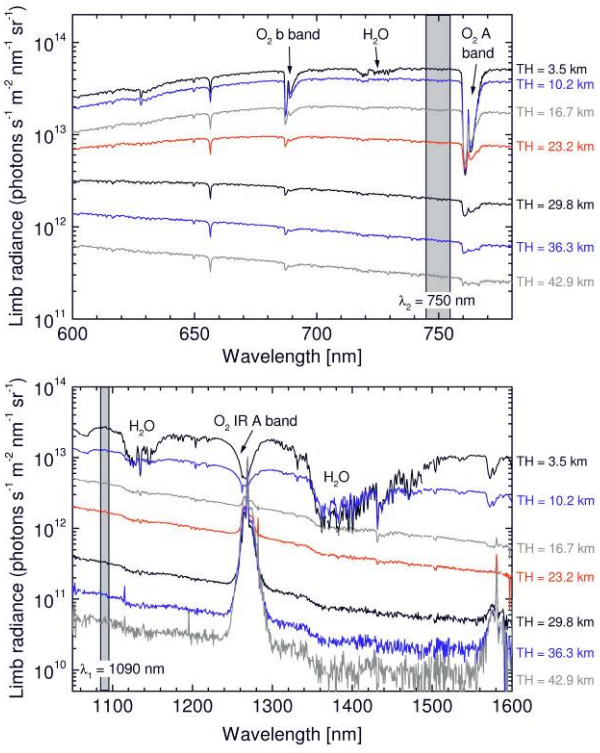

Fig. 1: Limb radiance spectra for SCIAMACHY channels 4 (upper panel) and 6 (lower panel) for a sample limb observation. Large radiances correspond to low tangent heights and vice versa. The most prominent feature in channel 4 is the O_2 A-band at 760 nm that appears as an absorption feature at low tangent heights and as an emission at higher tangent heights (not shown here).

$$R_c(TH) = \frac{I(TH, \lambda_1)}{I(TH, \lambda_2)}$$

In a second step the colour index ratio profile $\Theta(TH)$ between two adjacent tangent heights is determined from the colour index profiles:

$$\Theta(TH) = \frac{R_c(TH)}{R_c(TH + \Delta TH)}$$

with $\Delta TH \approx 3.3$ km being the SCIAMACHY tangent height step.

Fig. 2 shows colour index profiles $R_c(TH)$ and colour index ratio profiles $\Theta(TH)$ for two sample measurements with and without PSCs in the field of view. The use of the colour index ratio instead of the colour index itself has proven advantageous, since the colour index ratio can be forward-modelled with radiative transfer (RT) calculations even if the

measurements are not absolutely calibrated. As described in von *Savigny et al.* (2005a) radiative transfer simulations with the LIMBTRAN radiative transfer model were used as guidance for the determination of the PSC detection threshold. Based on these simulations as well as on empirical investigations – *i.e.* checking the occurrence of obvious false PSC detections – a PSC detection threshold value of Θ = 1.3 was employed. This implies that optically thin PSCs may not be detected, and the derived statistics may be somewhat biased to optically thicker PSCs. In order to avoid false PSC identifications due to cirrus clouds it is required that the enhancement in the colour index ratio has to occur at least 3 km above the climatological tropopause height taken from *Randel et al.* (2000). An advantage of the PSC detection method used here is that an additional temperature threshold (e.g., T < 200 K as in *Poole and Pitts* (1994)) does not have to be imposed. A more detailed description of the detection technique as well as the choices for the detection thresholds can be found in *von Savigny et al.* (2005a).

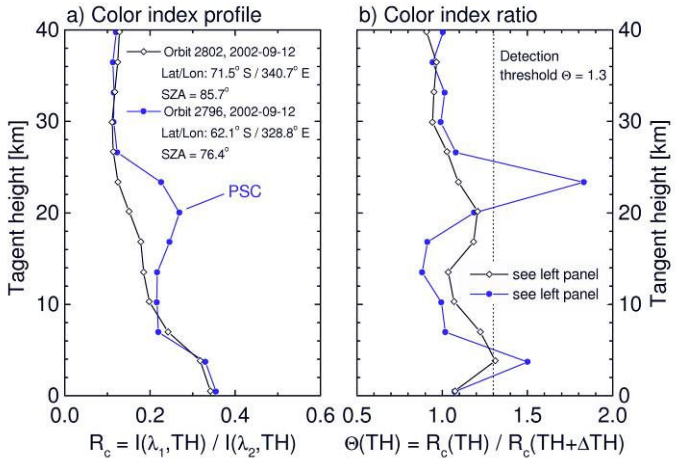

Fig. 2: Sample colour index profiles (left panel) and colour index ratio profiles (right panel) for SCIAMACHY limb scattering observations with and without PSCs in the field of view.

2. Auxiliary Data

Apart from the climatological tropopause height data set by *Randel et al.* (2000) no other auxiliary data is required for the detection of PSCs. The *Randel et al.* tropopause height climatology provides the latitudinal variation (in 5° latitude steps) of the tropopause height for each month of the year and is based on NCEP meteorological analyses.

3. Algorithm verification / validation

A validation of the PSC data product in a strict sense is difficult, because of the somewhat arbitrarily chosen PSC detection threshold. However, the thermal conditions under which PSC particles can form are very well established (*e.g.*, Peter, 1997). The formation of PSCs requires temperatures of less than about 195 K for PSC types Ia (NAT, nitric acid tri-hydrate; crystalline) and Ib (ternary solution of HNO_3, H_2SO_4 and H_2O; liquid), and less than about 188 K for PSC type II (H_2O ice). Therefore, checking the temperature at the location and altitude where PSCs are detected is a justified way to perform a verification of the PSC detection scheme. For this purpose temperature profiles for the location, date and time of each SCIAMACHY measurement were extracted from the ECMWF stratospheric analysis data set, and the temperatures at the altitude of the detected PSCs are determined. Fig. 3 shows histograms of the ECMWF temperature at PSC altitude for all PSCs detected in the southern hemisphere during the months of September of the years 2002 to 2009. Also indicated – as red vertical lines – are the approximate formation temperature thresholds for NAT PSCs and water ice or type II PSCs. Once can see that almost all of the detected PSCs occur at temperatures below about 195 – 198 K, the approximate PSC formation threshold. The mean temperatures vary slightly from year to year, but are always about 190 K. The fact that only a very small number of detections occur at temperatures above the expected PSC formation threshold provides a verification of the PSC detection method. Note that in September 2002,

e.g., the number of detected PSCs was quite low, which was a consequence of the unexpected major stratospheric warming in this month, which led to the disappearance of PSCs during the last week of September (*e.g., von Savigny et al.*, 2005b).

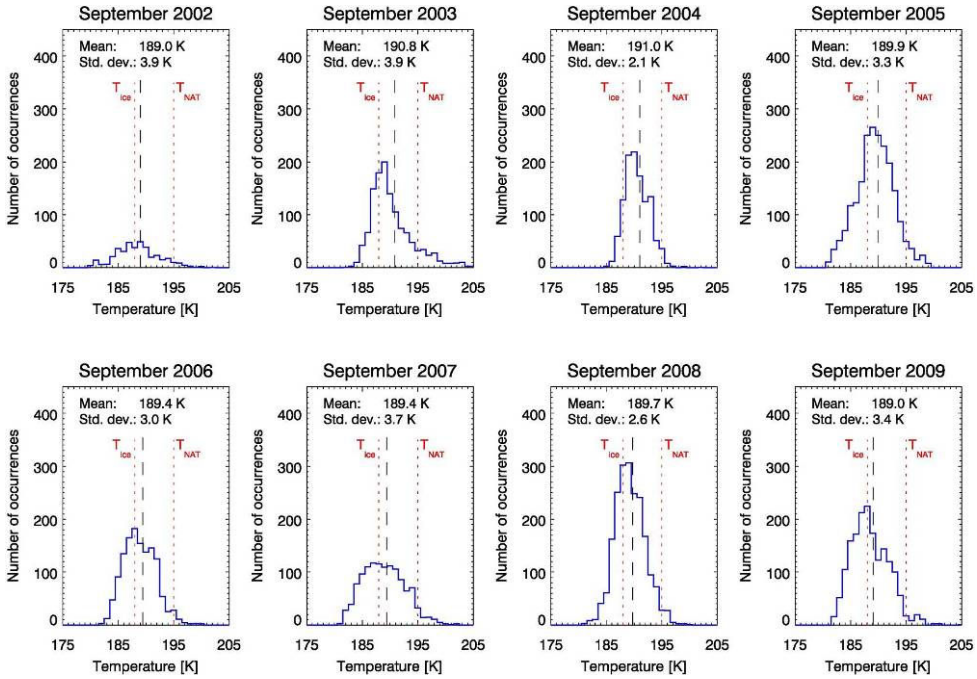

Fig. 3: Histograms of ECMWF temperature at the altitude and location of PSC detections in SCIAMACHY limb measurements for the southern hemisphere and the month of September of the years 2002 to 2009.

4. False PSC detections

Since the colour-index approach will capture any type of aerosol whose spectral dependence differs significantly from the Rayleigh spectral dependence, additional conditions may have to be imposed in order to avoid false PSC detections due to an enhanced stratospheric aerosol loading as a consequence of volcanic eruptions. The data set available on the www.iup.uni-bremen.de/scia-arc/ website was retrieved with a fixed colour index ratio threshold as described above.

Problems with false PSC detections due to volcanic aerosols occurred particularly for the northern hemisphere PSC seasons 2008/2009 and 2009/2010 as a consequence of the Kasatochi and Sarychev volcanic eruptions in 2008 and 2009, respectively. We also note that false PSC detections due to stratospheric background aerosol are expected to be more likely due to the small scattering angles of the SCIAMACHY limb-scatter observations at high northern latitudes (as small as about 25°). For high southern latitudes the scattering angles exceed 150°.

References:

Peter, T., Microphysics and heterogeneous chemistry of polar stratospheric clouds, ***Annu. Rev. Phys. Chem.***, 48, 785 – 822, 1997.

Poole, L. R., and Pitts, M. C.: Polar stratospheric cloud climatology based on stratospheric aerosol measurement II observations from 1978 to 1989, ***J. Geophys. Res.***, 99, 13,083 – 13,089, 1994.

Randel, W. J., Wu, W., and Gaffen, D.: Interannual variability of the tropical tropopause derived from radiosonde data and NCEP reanalyses, ***J. Geophys. Res.***, 105, 15,509 – 15,523, 2000.

von Savigny, C., Ulasi, E. P., Eichmann, K.-U., Bovensmann, H., and Burrows, J. P.: Detection and Mapping of Polar Stratospheric Clouds using Limb Scattering Observations, ***Atmos. Chem. Phys.***, 5, 3071 – 3079, www.atmos-chem-phys.org/acp/5/3071/, 2005a.

von Savigny, C., Rozanov, A., Bovensmann, H., Eichmann, K.-U., Noël, S., Rozanov, V. V., Sinnhuber, B.-M., Weber, M., and Burrows, J. P.: The ozone hole break-up in September 2002 as seen by SCIAMACHY on Envisat, ***J. Atmos. Sci.***, 62(3), 721 – 734, 2005b.